Editors' Suggestion

Nonequilibrium quasistationary spin disordered state in α-$RuCl_3$

R. B. Versteeg,[1,2] A. Chiocchetta,[3] F. Sekiguchi,[1] A. Sahasrabudhe,[1] J. Wagner,[1] A. I. R. Aldea,[1] K. Budzinauskas,[1] Zhe Wang,[1,4] V. Tsurkan,[5,6] A. Loidl,[5] D. I. Khomskii,[1] S. Diehl,[3] and P. H. M. van Loosdrecht[1,*]

[1]*Institute of Physics 2, Faculty of Mathematics and Natural Sciences, University of Cologne, Zülpicher Straße 77, D-50937 Cologne, Germany*

[2]*Laboratoire de Spectroscopie Ultrarapide and Lausanne Centre for Ultrafast Science (LACUS), ISIC-FSB, École Polytechnique Fédérale de Lausanne, CH-1015 Lausanne, Switzerland*

[3]*Institute for Theoretical Physics, University of Cologne, D-50937 Cologne, Germany*

[4]*Department of Physics, TU Dortmund University, Otto-Hahn-Straße 4, 44227 Dortmund, Germany*

[5]*Experimental Physics V, Center for Electronic Correlations and Magnetism, University of Augsburg, 86159 Augsburg, Germany*

[6]*Institute of Applied Physics, MD 2028, Chişinău, Republic of Moldova*

(Received 26 May 2021; revised 15 June 2022; accepted 16 June 2022; published 30 June 2022)

We photoexcite high-energy holon-doublon pairs as a way to alter the magnetic free energy landscape and resulting phase diagram of the frustrated honeycomb magnet α-$RuCl_3$. The pair recombination through multimagnon emission is tracked through the time evolution of the magnetooptical response originating from α-$RuCl_3$'s competing zigzag spin-ordered ground state. A small holon-doublon density suffices to reach a spin-disordered state. The phase transition is described within a dynamical Ginzburg-Landau framework, corroborating the quasistationary nature of the transient phase. Our work suggests a new route to reach a nontrivial spin-disordered state in Kitaev-like magnets.

DOI: 10.1103/PhysRevB.105.224428

I. INTRODUCTION

Light can be utilized as a tool to manipulate and engineer novel phases in quantum materials [1]. In particular, excitation via intense light pulses has been used to create nonequilibrium states of matter nonexistent at thermal equilibrium, such as transient superconductivity in underdoped cuprates [2], metastable ferroelectricity in $SrTiO_3$ [3,4], and unconventional charge-density wave order in $LaTe_3$ [5]. The light pulses excite a transient population of quasiparticles or collective excitations, which acts as a dynamical parameter to alter the material's free-energy landscape. For sufficiently strong excitation densities, a nonequilibrium phase transition can eventually occur [5–7]. By the same token, intense pulsed light holds promise to manipulate the spin state of frustrated magnets [8,9]. These materials, in fact, can host exotic and elusive phases, such as spin liquids (SL). Whereas SLs harbors rich many-body phenomena resulting from spin frustration and possible spin fractionalization [10,11], these phases often compete with a magnetically ordered ground state, which is typically energetically favored. Pulsed light excitation can then provide a mechanism to tip the energetic balance away from the magnetically ordered ground state towards a nonequilibrium spin-disordered phase with strong nontrivial magnetic correlations.

We explore this concept for the Kitaev-like frustrated magnet, a type of Mott insulator with a layered honeycomb structure and strong spin-orbit coupling [12–14]. For these materials the large spin-orbit interaction leads to a sizable bond directional spin exchange, whereas the symmetric Heisenberg exchange, in principle, cancels out by virtue of the edge-sharing octahedra geometry, making them promising candidates for Kitaev physics [12–14]. Still, the remaining Heisenberg and off-diagonal interaction, present due to small structural distortions away from the ideal honeycomb structure [15], is an adversary to spin-liquid formation, and generally favors a spin-ordered ground state [13,16,17]. By modulating spin entropy through finite temperature effects [18,19] or by adding external magnetic fields [20], one can, however, stabilize proximate or field-induced spin liquid phases at thermal equilibrium. These spin liquid realizations show the emergent behavior expected for the pure Kitaev spin liquid [10], most notably, fractionalized particle statistics [19] and quantized conduction phenomena [20].

A case in point is α-$RuCl_3$. This honeycomb Mott insulator has nearly ideal $j_{\text{eff}} = \frac{1}{2}$ isospins in highly symmetric octahedra [21,22], making it possibly the most promising Kitaev spin-liquid host studied to date [18–20]. The (B, T)-plane in Fig. 1 provides the *equilibrium* phase diagram as a function of magnetic field and temperature. Below the Néel temperature $T_N \approx 7\,\text{K}$, the isospins couple in a zigzag fashion, consistent with the types of magnetic order captured by the Kitaev-Heisenberg model [13]. Strong short-range spin correlations persist between T_N and the crossover temperature $T_H \approx 100\,\text{K}$, signalling the formation of a proximate spin liquid (pSL) phase within this intermediate temperature regime [18,23,24]. Above 100 K thermal fluctuations bring the system into a conventional paramagnetic phase. An additional tuning parameter is provided by an in-plane magnetic field. A field of $B_c \approx 7\,\text{T}$ is sufficient to destabilize the zigzag order. For fields between to 8 T a much-debated field-induced SL is then stabilized [20], whereas for higher fields a

*Corresponding author: pvl@ph2.uni-koeln.de

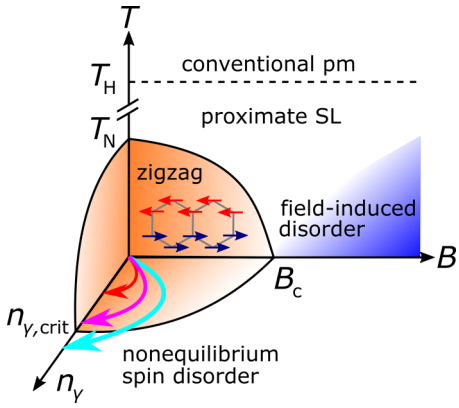

FIG. 1. The (B, T)-plane sketches α-$RuCl_3$'s *equilibrium* magnetic phase diagram. Photoexcited holon-doublon pairs n_γ form a new *nonequilibrium* parameter. For small (red) to intermediate (magenta) quenches the system stays inside the zigzag ordered phase. Above a critical density $n_{\gamma,\mathrm{crit}}$ a nonequilibrium spin-disordered state may be induced (light blue arrow).

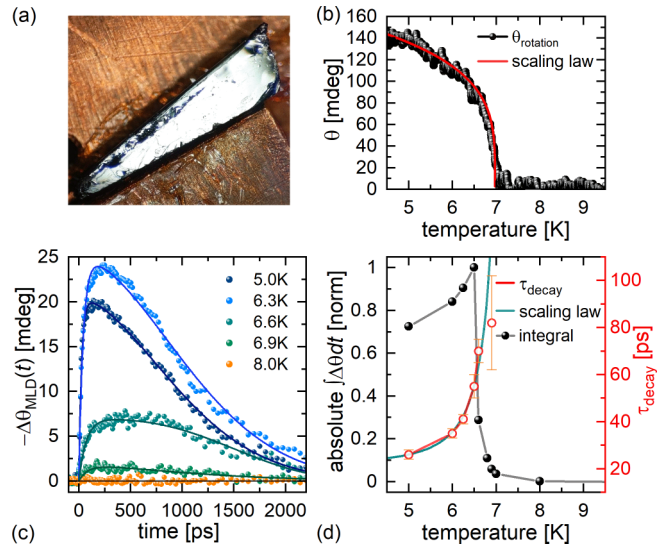

FIG. 2. (a) The shiny as-grown α-$RuCl_3$ sample used for this work. (b) The temperature-dependent magnetooptical response (black spheres) shows a clear scaling law behavior. A fit to $\theta_{\mathrm{MLD}} \propto L^2 \propto (1 - T/T_{\mathrm{N}})^{2\beta}$ with $\beta = 1/8$ is shown in red. (c) Photoinduced change in polarization rotation $-\Delta\theta_{\mathrm{MLD}}(t)$ for various temperatures below and above $T_{\mathrm{N}} \approx 7$ K. (d) Integrated change in rotation (black spheres) and τ_{decay} [ps] (red circles) as a function of temperature. A critical slowing down of the disordering is observed upon approaching the magnetic phase transition at $T_{\mathrm{N}} \approx 7$ K. The green curve shows a fit to the dynamical scaling-law behavior expected for α-$RuCl_3$.

quantum-disordered state with partial field alignment of the effective moments forms [15,25,26].

In this work, we report on the observation of a transient long-lived spin-disordered state in the frustrated honeycomb magnet α-$RuCl_3$ induced by pulsed light excitation. Holon-doublon pairs are created by photoexcitation above the Mott gap, and provide a new *nonequilibrium* dimension to α-$RuCl_3$'s magnetic free energy landscape and resulting phase diagram, as illustrated in Fig. 1. The subsequent holon-doublon pair recombination through multimagnon emission leads to a perturbation of the zigzag magnetic order. This is tracked through the magnetooptical response of the system, providing the dynamical evolution of the zigzag order parameter. For a sufficiently large holon-doublon density the magnetooptical response vanishes, showing that a long-lived transient spin-disordered phase is induced. The disordering dynamics is captured by a time-dependent Ginzburg-Landau model, corroborating the nonequilibrium quasistationary nature of the transient phase. The observations in α-$RuCl_3$ suggests a new route to induce an unconventional spin-disordered state in honeycomb Mott insulators with residual interactions beyond the bond-directional Kitaev exchange. More generally, the holon-doublon recombination-induced nonequilibrium quasistationary state description provides an advancement in the understanding of strongly correlated hot carrier recombination dynamics and nonequilibrium phase transitions in Mott-Hubbard insulator materials with intrinsically coupled charge and spin degrees of freedom.

II. ZIGZAG SPIN ORDER PARAMETER AND NEAR-EQUILIBRIUM MAGNETIZATION DYNAMICS

Before turning to the magnetization dynamics of α-$RuCl_3$, we establish its linear magnetooptical response as a probe of the zigzag spin order parameter. High-quality α-$RuCl_3$ crystals were prepared by vacuum sublimation [27,28]. For our work we used the as-grown shiny sample shown in Fig. 2(a). Figure 2(b) shows the optical polarization rotation upon reflection as a function of temperature, measured at 532-nm probe wavelength by a double-modulation scheme [29,30]. A magnetooptical response with clean power-law behavior is observed below $T_{\mathrm{N}} \approx 7$ K. The small structural monoclinicity can lead to an additional polarization rotation component, but this term appears to have a negligible contribution over the relevant temperature range of our study [15,31]. The magnetooptical rotation, more specifically, magnetic linear dichroism θ_{MLD}, is proportional to the square of the zigzag antiferromagnetic order parameter $\vec{L} = \vec{M}_\uparrow - \vec{M}_\downarrow$, where $\vec{M}_\uparrow$ and $\vec{M}_\downarrow$ give the sublattice magnetizations [32,33]. The red line in Fig. 2(b) shows a fit to the scaling law $\theta_{\mathrm{MLD}} \propto L^2 \propto (1 - T/T_{\mathrm{N}})^{2\beta}$, with $\beta = 1/8$ the critical exponent for a two-dimensional (2D) Ising spin system [34]. This observation establishes polarization spectroscopy as an all-optical alternative to neutron diffraction for probing α-$RuCl_3$'s zigzag spin order.

α-$RuCl_3$'s near-equilibrium magnetization dynamics is studied by weak photoexcitation and consecutive time-delayed probing of the change in the magnetooptical response for various bath temperatures. The sample is excited above the $\Delta_{\mathrm{MH}} \sim 1.0$ eV Mott-Hubbard gap [35] with a photon energy of $\hbar\omega \approx 1.55$ eV. A low pump fluence $F \approx 0.8\,\mu\mathrm{J\,cm^{-2}}$, corresponding to an excitation density of $n_\gamma \approx 0.4 \times 10^{17}\,\mathrm{cm^{-3}}$ was used [36]. Figure 2(c) displays the photoinduced change in polarization rotation $-\Delta\theta_{\mathrm{MLD}}(t)$, as measured by a polarization-dependent balanced detection scheme [29,37]. α-$RuCl_3$ shows spin-disordering dynamics on the tens of a ps timescale, followed by ns recovery dynamics below the Néel temperature $T_{\mathrm{N}} \approx 7$ K. Above T_{N} the

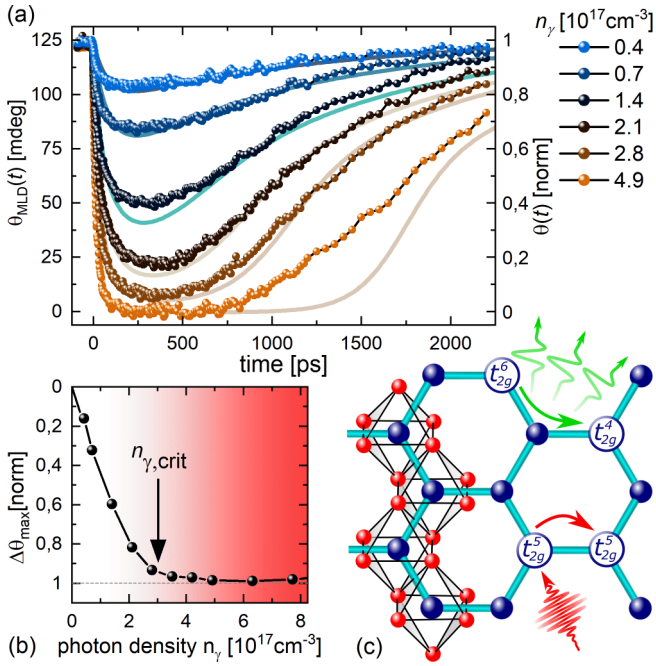

FIG. 3. (a) Density-dependent $\theta_{\mathrm{MLD}}(t)$ for different excitation densities n_γ, as indicated with spheres. The modeled rotation $\theta(t)$ is indicated with thick lines. (b) Maximum change in the magnetic linear dichroism (MLD) rotation $\Delta\theta_{\mathrm{MLD}}(t)$ as a function of photon density n_γ. Above the critical density $n_{\gamma,\mathrm{crit}} \approx 3\times10^{17}$ cm^{-3} the maximum change in MLD-rotation saturates. (c) The honeycomb lattice, consisting of Ru-sites (dark-blue sites) and chloride ligand ions (red sites). The lower process shows the photogeneration of a holon-doublon pair. The upper process shows the subsequent multimagnon emission by holon-doublon recombination.

transient response vanishes. The integrated transient response, plotted in Fig. 2(d), shows a pronounced increase, followed by a rapid reduction. This behavior is qualitatively rationalized by considering that the photoexcitation will have the largest transient effect where the derivative of the zigzag order parameter with respect to temperature is the largest. Concomitantly, we observe a slowing down of the disordering dynamics when approaching the equilibrium phase transition temperature [38,39]. The corresponding demagnetization time τ_{decay} is plotted in Fig. 2(d) [38,39]. The temperature dependence is well captured by a $\tau_{\mathrm{decay}} \propto |1 - T/T_{\mathrm{N}}|^{-\nu z}$ power law with critical exponent $\nu z = 2.1$, compatible with the universality class of the 2D Ising model-A dynamics, applicable to α-$RuCl_3$ [34,38,40]. Signatures of slowing down of the equilibrium magnetization dynamics in the zigzag-ordered phase were earlier observed in α-$RuCl_3$ and the related honeycomb iridate material Na_2IrO_3 through nuclear magnetic resonance spectroscopy [41,42].

III. NONEQUILIBRIUM SPIN-DISORDERED STATE AND EXCITATION MECHANISM

Strong photoexcitation allows one to induce a magnetic order-disorder transition along a nonequilibrium route. Figure 3(a) shows the transient rotation traces $\theta_{\mathrm{MLD}}(t)$ for various initial photoexcitation densities n_γ (sphere symbols) at a bath temperature of $T_{\mathrm{bath}} = 5$ K [36]. The photoexcitation dependence of the maximum MLD change, $\Delta\theta_{\mathrm{MLD,max}}$, is depicted in Fig. 3(b). Markedly different dynamics is observed compared to crossing the order-disorder transition along the equilibrium axis [cf. Fig. 2(c)]. Qualitatively, two excitation regimes can be distinguished. For lower excitation densities ($n_\gamma < n_{\gamma,\mathrm{crit}} \approx 3\times10^{17}\,\mathrm{cm}^{-3}$), the spin system partially disorders, followed by a subsequent recovery. In this regime the disordering time slows down with increasing photoexcitation density. For the high excitation densities ($n_\gamma > n_{\gamma,\mathrm{crit}} \approx 3\times10^{17}\,\mathrm{cm}^{-3}$) a faster disordering time is observed and the change $\Delta\theta_{\mathrm{MLD,max}}$ saturates to a value of ≈ -125 mdeg [Fig. 3(b)]. This transient disorder magnitude agrees well with the value expected from the equilibrium rotation measurement [Fig. 2(b)]. These observations thus imply that the photoexcited system resides in a $L = 0$ state for multiple 100s of ps. Referring to the magnetic phase diagram (Fig. 1 and Refs. [15,20]), this means that for quench strengths above $n_{\gamma,\mathrm{crit}}$ the zigzag order can be fully suppressed, leaving the system in a spin-disordered state. The disordering mechanism and the nature of the long-lived transient state is corroborated below.

Strong photoexcitation allows one to induce a magnetic order-disorder transition along a nonequilibrium route. Figure 3(a) shows the transient rotation traces $\theta_{\mathrm{MLD}}(t)$ for various initial photoexcitation densities n_γ (sphere symbols) at a bath temperature of $T_{\mathrm{bath}} = 5$ K [36]. The photoexcitation dependence of the maximum MLD change, $\Delta\theta_{\mathrm{MLD,max}}$, is depicted in Fig. 3(b). Markedly different dynamics is observed compared to crossing the order-disorder transition along the equilibrium axis [cf. Fig. 2(c)]. Qualitatively, two excitation regimes can be distinguished. For lower excitation densities ($n_\gamma < n_{\gamma,\mathrm{crit}} \approx 3\times10^{17}\,\mathrm{cm}^{-3}$), the spin system partially disorders, followed by a subsequent recovery. In this regime the disordering time slows down with increasing photoexcitation density. For the high excitation densities ($n_\gamma > n_{\gamma,\mathrm{crit}} \approx 3\times10^{17}\,\mathrm{cm}^{-3}$) a faster disordering time is observed and the change $\Delta\theta_{\mathrm{MLD,max}}$ saturates [Fig. 3(b)], implying that the photoexcited system resides in a $L = 0$ state for multiple 100s of ps. Referring to the magnetic phase diagram (Fig. 1 and Refs. [15,20]), this means that for quench strengths above $n_{\gamma,\mathrm{crit}}$ the zigzag order can be fully suppressed, leaving the system in a spin-disordered state. The disordering mechanism and the nature of the long-lived transient state is corroborated below.

The inherently strong charge-spin coupling of Mott insulators leads to an efficient nonlinear demagnetization mechanism upon photoexcitation above the Mott-Hubbard gap [43,44]. To illustrate this mechanism, first consider the photoexcitation process corresponding to the lowest $t_{2g}^5 t_{2g}^5 \rightarrow t_{2g}^4 t_{2g}^6$ hopping-type excitation across the Mott-Hubbard gap, as indicated by the lower hopping process in Fig. 3(c). Within a quasiparticle picture, this intermediate excited state corresponds to a spinless *holon* (t_{2g}^4) and *doublon* (t_{2g}^6), by which effectively two magnetic moments are removed from the zigzag lattice. Their mere creation at the used low densities of 4–85 ppm photons/Ru^{3+}-site, however, does not suffice to explain the magnitude and timescale of the zigzag disordering [36]. Instead, once created, the dominant pair-decay mechanism is *recombination* through multimagnon emission

[upper hopping process Fig. 3(c)] [43]. An order of magnitude estimate for the released amount of magnons per decayed *hd*-pair (holon-doublon pair) is provided by $\Delta_{\mathrm{MH}}/W \sim 40$ (Ref. [43]), with $W \approx 25$ meV the exchange energyscale, estimated as the extent of α-$RuCl_3$'s magnetic scattering continuum [19,24,26]. The holon-doublon recombination by multimagnon emission therefore provides an efficient electronic demagnetization mechanism.

To further delineate the excitation mechanism and resulting magnetization dynamics, we model the time-domain data within a dynamical Ginzburg-Landau (GL) model [38,40]. The holon-doublon density, representing the nonequilibrium dimension in Fig. 1, comes in as a new dynamical variable here. We first consider the modified free energy for the antiferromagnetic order parameter L and the holon-doublon-*pair* density n:

$$\mathcal{F}(n, L) = \frac{a_1}{2}(n - n_{\mathrm{c,eq}})L^2 + \frac{a_2}{4}L^4 + \tilde{\mathcal{F}}(n), \tag{1}$$

with

$$\tilde{\mathcal{F}}(n) = a_3 n + \frac{a_4}{2}n^2 + \frac{a_5}{3}n^3, \tag{2}$$

where a_i, $i = 1, \ldots, 5$ are phenomenological parameters. The terms with even powers in the zigzag order parameter L are the symmetry-allowed terms in the Landau free-energy expansion for an antiferromagnet [40,45]. Notice that odd powers of L are ruled out by the inversion symmetry of α-$RuCl_3$ [15]. The initial value of the holon-doublon pair density $n(0)$, or quench strength, is taken proportional to the experimental photoexcitation densities n_γ, i.e., $n(0) \propto n_\gamma$, where each photon creates one *hd*-pair. The first term in $\mathcal{F}(n, L)$, coupling the *hd*-pair density n to the order parameter L, leads to a destabilization of the magnetic order for a sufficiently strong excitation of *hd*-pairs, thus reproducing the process of annihilation of *hd*-pairs into magnons [43,46]. The parameter $n_{\mathrm{c,eq}}$ is introduced as the critical *hd*-pair density at equilibrium. The functional $\tilde{\mathcal{F}}(n)$, independent of the order parameter L, describes the excess energy of the *hd*-density and its relaxation in the absence of magnetization. It therefore accounts for decay mechanisms other than the nonradiative multimagnon emission discussed above, such as nonradiative phonon emission, spontaneous decay under radiative emission [47], and possible *hd*-pair diffusion out of the probe volume. The form of $\tilde{\mathcal{F}}(n)$ is chosen as a third-order polynomial, although its exact form is not crucial for the analysis.

The time evolution of the *hd*-pair density n and magnetic order parameter L is described by the coupled equations of motion

$$\frac{dL}{dt} = -\frac{\delta \mathcal{F}}{\delta L}, \quad \frac{dn}{dt} = -\frac{\delta \mathcal{F}}{\delta n}. \tag{3}$$

To relate Eqs. (3) to the experimentally measured rotation θ_{MLD}, we rewrite the equations in terms of the polarization rotation $\theta = L^2/2$, to finally obtain

$$\frac{d\theta}{dt} = -2a_1(n - n_{\mathrm{c,eq}})\theta - 4a_2\theta^2, \tag{4a}$$

$$\frac{dn}{dt} = -a_1\theta - \frac{\delta}{\delta n}\tilde{\mathcal{F}}(n). \tag{4b}$$

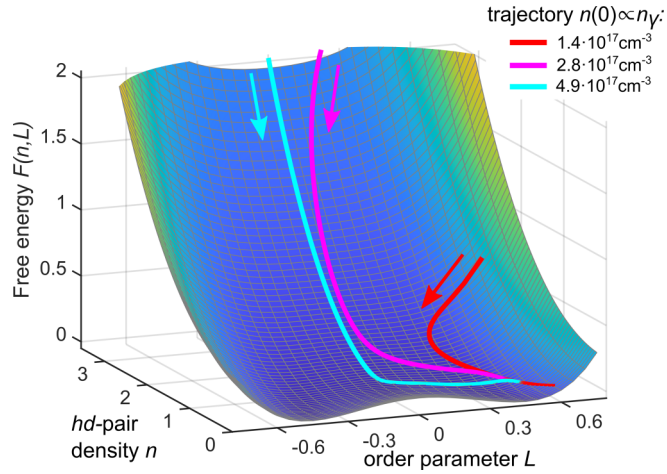

FIG. 4. Free-energy landscape $F(n, L)$ as a function of the zigzag order parameter L and *hd*-pair density n (cf. the phase diagram in Fig. 1). The initial quench $n(0)$ brings the system to a high-energy state, after which the system relaxes. For small quenches (red trajectory), the order parameter L stays finite under the relaxation of the density n. For intermediate quenches (magenta trajectory) the system approaches the $L = 0$ line. For strong quenches (light blue trajectory, highest energies not shown) the system relaxes along the $L = 0$ line, implying that the system is described as a nonequilibrium quasistationary spin-disordered state.

By using Eq. (4a), the trajectories $n(t), \theta(t)$ can be modeled for different initial quench strengths $n(0)$, taken proportional to the experimental n_γ densities. The curves for $\theta(t)$ are superimposed on the experimental $\theta_{\mathrm{MLD}}(t)$ in Fig. 3(a). The model captures the dynamical slowing down and speeding up below and above $n_{\gamma,\mathrm{crit}}$, respectively. For the higher excitation densities the magnetic order vanishes, reproducing the long-lived transient $L = 0$ state. The inclusion of the n^3-term in $\tilde{\mathcal{F}}(n)$ ensures that the GL description does not overestimate the lifetime of the disordered state [48]. The nonlinear order parameter dynamics is overall well captured considering the minimal amount of parameters needed in the nonequilibrium GL description.

The out-of-equilibrium nature of the spin-disordered phase is best visualized in the *hd*-pair density-dependent free-energy landscape $\mathcal{F}(n, L)$ of Fig. 4. For low densities, the free energy retains its double-well profile, whereas for higher densities a single well forms [39]. Representative trajectories $n(t), L(t)$ for different excitation densities are drawn into the free-energy landscape, with colors corresponding to the conceptual trajectories of Fig. 1. The quench $n(0)$ brings the system into a high-energy state, after which n and L relax along the minimal energy trajectory. For a small quench (red trajectory) the zigzag order parameter $L(t)$ stays finite and eventually recovers. For the intermediate densities (magenta trajectory) the $n(t), L(t)$ coordinates approach the $L = 0$ line. For the higher excitation densities (light blue trajectory) the *hd*-pairs have sufficient excess energy to let $n(t), L(t)$ follow a trajectory along the $L = 0$ line, i.e., full spin disordering is reached. We emphasize that, for strong quenches, the excitation density $n(t)$ still varies in time, even though $L(t)$ takes the quasistationary value $L(t) = 0$. A sufficiently strong photoexcitation

quench thus provides a mechanism to induce a *nonequilibrium quasistationary* spin-disordered state in α-$RuCl_3$.

The maximum lifetime of the nonequilibrium quasistationary spin-disordered state is dictated by the recombination rate of the *hd*-pairs. The time evolution of $n(t)$ obtained from the nonequilibrium GL model provides us with an estimate of a few nanoseconds for the recombination timescale of the *hd*-pairs [48], in agreement with the long electronic relaxation timescale observed by time-resolved photoemission [49]. The recombination timescale is expected to grow exponentially with the number of magnons needed to traverse the Mott gap, i.e., $\tau \sim e^{\Delta_{\mathrm{MH}}/W}$ [43]. Considering the weak exchange-interaction scale W in α-$RuCl_3$, one may indeed expect significantly longer recombination times compared to materials with an order of magnitude stronger exchange, such as Nd_2CuO_4 and Sr_2IrO_4, where *hd*-pair lifetimes on the order of 0.1 ps were reported [44,50]. In addition to the common interaction mechanisms which extend the lifetime of transient electronic carriers, such as carrier dressing by phonons [51], the large ratio between the Mott gap and the exchange interaction energy thus emerges as the key element to ensure a long lifetime of the nonequilibrium quasistationary state.

Consensus crystallizes towards an understanding of α-$RuCl_3$'s equilibrium disordered phase above T_N as a realization of a proximate quantum spin liquid [14,18,23]. Since the used low photoexcitation densities in our study are by far not sufficient to drive α-$RuCl_3$ into a conventional paramagnetic state along purely equilibrium thermodynamics arguments [28,52], it appears plausible that the nonequilibrium quasistationary-disordered phase has a microscopic character reminiscent of the equilibrium proximate spin-liquid phase. We envision the use of time-resolved inelastic light scattering techniques as a powerful method to probe magnetic correlations in the out-of-equilibrium spin *disordered* phase [19,53]. Exact diagonalization [54] and nonequilibrium dynamical mean-field theory [55,56] methods may elucidate the role of *hd*-excitations in the Kitaev-Heisenberg model and the resulting phase diagram, and hence further resolve our findings from a microscopic viewpoint.

IV. CONCLUSION

In conclusion, we unveiled a pulsed light excitation driven mechanism allowing to trap the frustrated honeycomb magnet α-$RuCl_3$ into a nonequilibrium quasistationary spin disordered state. Photoexcitation above the Mott-gap generates a transient density of holon-doublon quasiparticle pairs. The subsequent pair-recombination through multimagnon emission provides a way to dynamically destabilize α-$RuCl_3$'s competing zigzag-ordered ground state, and thereby keeps the system in a long-lived out-of-equilibrium spin-disordered state. Our findings suggest a new route to induce an unconventional spin-disordered state in honeycomb Mott insulators with residual interactions beyond the bond-directional Kitaev exchange. The insights to hot carrier recombination dynamics and nonequilibrium phase transition kinetics in a strongly correlated environment are expected to be extendable to a large class of Mott-Hubbard insulator materials with strong charge-spin coupling.

ACKNOWLEDGMENTS

The authors thank A. Rosch (Cologne, DE), C. Hickey (Cologne, DE), and Z. Lenarčič (Berkeley, USA) for fruitful discussions. This project was partially financed by the Deutsche Forschungsgemeinschaft (DFG) through Project No. 277146847—Collaborative Research Center 1238: Control and Dynamics of Quantum Materials (Subprojects No. B05 and No. C04) and through Project No. INST 216/783-1 FUGG. S.D. acknowledges support by the European Research Council (ERC) under the Horizon 2020 research and innovation program, Grant Agreement No. 647434 (DOQS).

[1] D. N. Basov, R. D. Averitt, and D. Hsieh, Towards properties on demand in quantum materials, Nat. Mater. **16**, 1077 (2017).

[2] D. Fausti, R. I. Tobey, N. Dean, S. Kaiser, A. Dienst, M. C. Hoffmann, S. Pyon, T. Takayama, H. Takagi, and A. Cavalleri, Light-induced superconductivity in a stripe-ordered cuprate, Science **331**, 189 (2011).

[3] T. F. Nova, A. S. Disa, M. Fechner, and A. Cavalleri, Metastable ferroelectricity in optically strained $SrTiO_3$, Science **364**, 1075 (2019).

[4] X. Li, T. Qiu, J. Zhang, E. Baldini, J. Lu, A. M. Rappe, and K. A. Nelson, Terahertz field-induced ferroelectricity in quantum paraelectric $SrTiO_3$, Science **364**, 1079 (2019).

[5] A. Kogar, A. Zong, P. E. Dolgirev, X. Shen, J. Straquadine, Y.-Q. Bie, X. Wang, T. Rohwer, I-C. Tung, Y. Yang, R. Li, J. Yang, S. Weathersby, S. Park, M. E. Kozina, E. J. Sie, H. Wen, P. Jarillo-Herrero, I. R. Fisher, X. Wang *et al.*, Light-induced charge density wave in $LaTe_3$, Nat. Phys. **16**, 159 (2020).

[6] S. W. Teitelbaum, B. K. Ofori-Okai, Y.-H. Cheng, J. Zhang, F. Jin, W. Wu, R. D. Averitt, and K. A. Nelson, Dynamics of a Persistent Insulator-to-Metal Transition in Strained Manganite Films, Phys. Rev. Lett. **123**, 267201 (2019).

[7] P. E. Dolgirev, M. H. Michael, A. Zong, N. Gedik, and E. Demler, Self-similar dynamics of order parameter fluctuations in pump-probe experiments, Phys. Rev. B **101**, 174306 (2020).

[8] L. Balents, Spin liquids in frustrated magnets, Nature (London) **464**, 199 (2010).

[9] J. Knolle and R. Moessner, A field guide to spin liquids, Annu. Rev. Condens. Matter Phys. **10**, 451 (2019).

[10] A. Kitaev, Anyons in an exactly solved model and beyond, Ann. Phys. (NY) **321**, 2 (2006).

[11] C. Broholm, R. J. Cava, S. A. Kivelson, D. G. Nocera, M. R. Norman, and T. Senthil, Quantum spin liquids, Science **367**, eaay0668 (2020).

[12] G. Jackeli and G. Khaliullin, Mott Insulators in the Strong Spin-Orbit Coupling Limit: From Heisenberg to a Quantum Compass and Kitaev Models, Phys. Rev. Lett. **102**, 017205 (2009).

[13] J. Chaloupka, G. Jackeli, and G. Khaliullin, Zigzag Magnetic Order in the Iridium Oxide Na_2IrO_3, Phys. Rev. Lett. **110**, 097204 (2013).

[14] H. Takagi, T. Takayama, G. Jackeli, G. Khaliullin, and S. E. Nagler, Concept and realization of Kitaev quantum spin liquids, Nat. Rev. Phys. **1**, 264 (2019).

[15] R. D. Johnson, S. C. Williams, A. A. Haghighirad, J. Singleton, V. Zapf, P. Manuel, I. I. Mazin, Y. Li, H. O. Jeschke, R. Valentí, and R. Coldea, Monoclinic crystal structure of α-$RuCl_3$ and the zigzag antiferromagnetic ground state, Phys. Rev. B **92**, 235119 (2015).

[16] Z. Alpichshev, F. Mahmood, G. Cao, and N. Gedik, Confinement-Deconfinement Transition as an Indication of Spin-Liquid-Type Behavior in Na_2IrO_3, Phys. Rev. Lett. **114**, 017203 (2015).

[17] N. Nembrini, S. Peli, F. Banfi, G. Ferrini, Yogesh Singh, P. Gegenwart, R. Comin, K. Foyevtsova, A. Damascelli, A. Avella, and C. Giannetti, Tracking local magnetic dynamics via high-energy charge excitations in a relativistic Mott insulator, Phys. Rev. B **94**, 201119(R) (2016).

[18] S.-H. Do, S.-Y. Park, J. Yoshitake, J. Nasu, Y. Motome, Y. Seung Kwon, D. T. Adroja, D. J. Voneshen, K. Kim, T.-H. Jang, J.-H. Park, K.-Y. Choi, and S. Ji, Majorana fermions in the Kitaev quantum spin system α-$RuCl_3$, Nat. Phys. **13**, 1079 (2017).

[19] L. J. Sandilands, Y. Tian, K. W. Plumb, Y.-J. Kim, and K. S. Burch, Scattering Continuum and Possible Fractionalized Excitations in α-$RuCl_3$, Phys. Rev. Lett. **114**, 147201 (2015).

[20] Y. Kasahara, T. Ohnishi, Y. Mizukami, O. Tanaka, S. Ma, K. Sugii, N. Kurita, H. Tanaka, J. Nasu, Y. Motome, T. Shibauchi, and Y. Matsuda, Majorana quantization and half-integer thermal quantum hall effect in a Kitaev spin liquid, Nature (London) **559**, 227 (2018).

[21] K. W. Plumb, J. P. Clancy, L. J. Sandilands, V. Vijay Shankar, Y. F. Hu, K. S. Burch, H.-Y. Kee, and Y.-J. Kim, α-$RuCl_3$: A spin-orbit assisted Mott insulator on a honeycomb lattice, Phys. Rev. B **90**, 041112(R) (2014).

[22] S. Agrestini, C.-Y. Kuo, K.-T. Ko, Z. Hu, D. Kasinathan, H. B. Vasili, J. Herrero-Martin, S. M. Valvidares, E. Pellegrin, L.-Y. Jang, A. Henschel, M. Schmidt, A. Tanaka, and L. H. Tjeng, Electronically highly cubic conditions for Ru in α-$RuCl_3$, Phys. Rev. B **96**, 161107(R) (2017).

[23] A. Banerjee, C. A. Bridges, J.-Q. Yan, A. A. Aczel, L. Li, M. B. Stone, G. E Granroth, M. D. Lumsden, Y. Yiu, J. Knolle, S. Bhattacharjee, D. L. Kovrizhin, R. Moessner, D. A. Tennant, D. G. Mandrus, and S. E. Nagler, Proximate Kitaev quantum spin liquid behaviour in a honeycomb magnet, Nat. Mater. **15**, 733 (2016).

[24] S. M. Winter, K. Riedl, D. Kaib, R. Coldea, and R. Valentí, Probing α-$RuCl_3$ beyond Magnetic Order: Effects of Temperature and Magnetic Field, Phys. Rev. Lett. **120**, 077203 (2018).

[25] J. A. Sears, Y. Zhao, Z. Xu, J. W. Lynn, and Y.-J. Kim, Phase diagram of α-$RuCl_3$ in an in-plane magnetic field, Phys. Rev. B **95**, 180411(R) (2017).

[26] A. Sahasrabudhe, D. A. S. Kaib, S. Reschke, R. German, T. C. Koethe, J. Buhot, D. Kamenskyi, C. Hickey, P. Becker, V. Tsurkan, A. Loidl, S. H. Do, K. Y. Choi, M. Grüninger, S. M. Winter, Zhe Wang, R. Valentí, and P. H. M. van Loosdrecht. High-field quantum disordered state in α-$RuCl_3$: Spin flips, bound states, and multiparticle continuum, Phys. Rev. B **101**, 140410(R) (2020).

[27] See Supplemental Material at http://link.aps.org/supplemental/10.1103/PhysRevB.105.224428 for information regarding the sample growth and preparation.

[28] H. B. Cao, A. Banerjee, J.-Q. Yan, C. A. Bridges, M. D. Lumsden, D. G. Mandrus, D. A. Tennant, B. C. Chakoumakos, and S. E. Nagler, Low-temperature crystal and magnetic structure of α-$RuCl_3$, Phys. Rev. B **93**, 134423 (2016).

[29] See Supplemental Material at http://link.aps.org/supplemental/10.1103/PhysRevB.105.224428 for information regarding the steady-state and time-resolved magnetooptical experimental techniques.

[30] K. Sato, Measurement of Magneto-optical Kerr effect using piezo-birefringent modulator, Jpn. J. Appl. Phys. **20**, 2403 (1981).

[31] A. Glamazda, P. Lemmens, S.-H. Do, Y. S. Kwon, and K.-Y. Choi, Relation between Kitaev magnetism and structure in α-$RuCl_3$, Phys. Rev. B **95**, 174429 (2017).

[32] G. A. Smolenskiĭ, R. V. Pisarev, and I. G. Sinii, Birefringence of light in magnetically ordered crystals, Sov. Phys. Usp. **18**, 410 (1975).

[33] R. V. Pisarev, B. B. Krichevtsov, and V. V. Pavlov, Optical study of the antiferromagnetic-paramagnetic phase transition in chromium oxide Cr_2O_3, Phase Trans. **37**, 63 (1991).

[34] A. Banerjee, J. Yan, J. Knolle, C. A. Bridges, M. B.Stone, M. D. Lumsden, D. G. Mandrus, D. A. Tennant, R. Moessner, and S. E. Nagler, Neutron scattering in the proximate quantum spin liquid α-$RuCl_3$, Science **356**, 1055 (2017).

[35] L. J. Sandilands, C. H. Sohn, H. J. Park, S. Yeun Kim, K. W. Kim, J. A. Sears, Y.-J. Kim, and T. Won Noh, Optical probe of Heisenberg-Kitaev magnetism in α-$RuCl_3$, Phys. Rev. B **94**, 195156 (2016).

[36] See Supplemental Material at http://link.aps.org/supplemental/10.1103/PhysRevB.105.224428 for more details on the determination of the photoexcitation density.

[37] J. Wang, in *Optical Techniques for Solid-State Materials Characterization*, edited by R. P. Prasankumar and A. J. Taylor (CRC, Boca Raton, FL, 2012), Chap. 13.

[38] P. C. Hohenberg and B. I. Halperin, Theory of dynamic critical phenomena, Rev. Mod. Phys. **49**, 435 (1977).

[39] A. Zong, P. E. Dolgirev, A. Kogar, E. Ergeçen, M. B. Yilmaz, Y.-Q. Bie, T. Rohwer, I-C. Tung, J. Straquadine, X. Wang, Y. Yang, X. Shen, R. Li, J. Yang, S. Park, M. C. Hoffmann, B. K. Ofori-Okai, M. E. Kozina, H. Wen, X. Wang *et al.*, Dynamical Slowing-Down in an Ultrafast Photoinduced Phase Transition, Phys. Rev. Lett. **123**, 097601 (2019).

[40] U. C. Täuber, *Critical Dynamics: A Field Theory Approach to Equilibrium and Non-Equilibrium Scaling Behavior* (Cambridge University Press, Cambridge, England, 2014).

[41] S. K. Takahashi, J. Wang, A. Arsenault, T. Imai, M. Abramchuk, F. Tafti, and P. M. Singer, Spin Excitations of a Proximate Kitaev Quantum Spin Liquid Realized in Cu_2IrO_3, Phys. Rev. X **9**, 031047 (2019).

[42] N. Janša, A. Zorko, M. Gomilšek, M. Pregelj, K. W. Krämer, D. Biner, A. Biffin, C. Rüegg, and M. Klanjšek, Observation of two types of fractional excitation in the Kitaev honeycomb magnet, Nat. Phys. **14**, 786 (2018).

[43] Z. Lenarčič and P. Prelovšek, Ultrafast Charge Recombination in a Photoexcited Mott-Hubbard Insulator, Phys. Rev. Lett. **111**, 016401 (2013).

[44] D. Afanasiev, A. Gatilova, D. J. Groenendijk, B. A. Ivanov, M. Gibert, S. Gariglio, J. Mentink, J. Li, N. Dasari, M. Eckstein, Th. Rasing, A. D. Caviglia, and A. V. Kimel, Ultrafast Spin Dynamics in Photodoped Spin-Orbit Mott Insulator Sr_2IrO_4, Phys. Rev. X **9**, 021020 (2019).

[45] D. I. Khomskii, *Basic Aspects of the Quantum Theory of Solids: Order and Elementary Excitations* (Cambridge University Press, Cambridge, England, 2010).

[46] See Supplemental Material at http://link.aps.org/supplemental/10.1103/PhysRevB.105.224428 for the derivation of the effective coupling $\propto nL^2$ between the holon-doublon density and antiferromagnetic order parameter from the microscopic Hamiltonian discussed in Ref. [43]

[47] M. Mitrano, G. Cotugno, S. R. Clark, R. Singla, S. Kaiser, J. Stähler, R. Beyer, M. Dressel, L. Baldassarre, D. Nicoletti, A. Perucchi, T. Hasegawa, H. Okamoto, D. Jaksch, and A. Cavalleri, Pressure-Dependent Relaxation in the Photoexcited Mott insulator ET $-$ F_2TCNQ: Influence of Hopping and Correlations on Quasiparticle Recombination Rates, Phys. Rev. Lett. **112**, 117801 (2014).

[48] See Supplemental Material at http://link.aps.org/supplemental/10.1103/PhysRevB.105.224428 for more details on the time-dependent Ginzburg-Landau model.

[49] D. Nevola, A. Bataller, A. Kumar, S. Sridhar, J. Frick, S. O'Donnell, H. Ade, P. A. Maggard, A. F. Kemper, K. Gundogdu, and D. B. Dougherty, Timescales of excited state relaxation in α-$RuCl_3$ observed by time-resolved two-photon photoemission spectroscopy, Phys. Rev. B **103**, 245105 (2021)

[50] H. Okamoto, T. Miyagoe, K. Kobayashi, H. Uemura, H. Nishioka, H. Matsuzaki, A. Sawa, and Y. Tokura, Photoinduced transition from Mott insulator to metal in the undoped cuprates Nd_2CuO_4 and La_2CuO_4, Phys. Rev. B **83**, 125102 (2011).

[51] P. Werner and M. Eckstein, Field-induced polaron formation in the Holstein-Hubbard model, Europhys. Lett. **109**, 37002 (2015).

[52] See Supplemental Material at http://link.aps.org/supplemental/10.1103/PhysRevB.105.224428 for the thermodynamic approach to describe the phase transition.

[53] G. B. Halász, N. B. Perkins, and J. van den Brink, Resonant Inelastic X-Ray Scattering Response of the Kitaev Honeycomb Model, Phys. Rev. Lett. **117**, 127203 (2016).

[54] S. Okamoto, Global phase diagram of a doped Kitaev-Heisenberg model, Phys. Rev. B **87**, 064508 (2013).

[55] H. Aoki, N. Tsuji, M. Eckstein, M. Kollar, T. Oka, and P. Werner, Nonequilibrium dynamical mean-field theory and its applications, Rev. Mod. Phys. **86**, 779 (2014).

[56] J. Li and M. Eckstein, Nonequilibrium steady-state theory of photodoped Mott insulators, Phys. Rev. B **103**, 045133 (2021).